

Gauss-Newton Method in the Problem of Optimizing the Axisymmetric Phase Function Calculation Based on the Hilbert Diagnostic Data

E.V. Arbuzov^{1,A,B}, V.A. Arbuzov^{2,A}, Yu.N. Dubnishchev^{3,A}, O.S. Zolotukhina^{4,A}

^A Kutateladze Institute of Thermophysics of the Siberian Branch of the Russian Academy of Sciences

^B Sobolev Institute of Mathematics of the Siberian Branch of the Russian Academy of Sciences

¹ ORCID: 0000-0001-9488-8650, arbuzov@math.nsc.ru

² ORCID: 0000-0003-2404-326X, arbuzov@itp.nsc.ru

³ ORCID: 0000-0001-7874-039X, dubnistchev@itp.nsc.ru

⁴ ORCID: 0000-0003-3486-4459, melexina-olga17@yandex.ru

Abstract

A method for reconstructing phase disturbances of a probing light field using the iterative Gauss-Newton algorithm is discussed as part of the Hilbert diagnostics development of gaseous, condensed and reacting media. In this case, the need to determine second derivatives is eliminated, which simplifies the calculations. The method consists of selecting a phase profile, which is specified by a Bezier curve, and hilbertogram calculating. The coincidence of the reference and reconstructed hilbertograms serves as a criterion for the results reliability. The Jacobian matrix for the nonlinear integral operator of Hilbert visualization is obtained. The algorithm is analyzed using a test function. The method development is associated with the algorithm application to the processing of experimental results, including the reconstruction of complex structures in which the phase function is described by several Bezier polynomials.

Keywords: Hilbert optics, phase function, optimization, Gauss-Newton method.

1. Introduction

The Hilbert diagnostics of phase structures is the important result of a fruitful synthesis of methods developed in optics and radio engineering [1, 2]. This is an integral operation that signal energy redistributes in a given band of spatial frequencies of the probing field perturbed by the medium under study. The energy loss of the optical signal is minimized in this case. The Hilbert transform in the frequency space is reduced to a certain type of phase transformation of the signal Fourier spectrum with energy conservation in a wide frequency band.

The Hilbert diagnostics results of reacting jets were previously presented in [3, 4]. The possibility of polychromatic Hilbert visualization of phase optical density fields with temperature profile measurement in selected sections of the medium under study is shown using the example of an axisymmetric hydrogen-air diffusion flame and a candle flame using the Abel transform. Iterative selection of radial temperature profiles fitted by Bezier curves, followed by spatial structure calculation of the refractive index and phase function, is performed. Comparison of hilbertograms obtained in the experiment with hilbertograms modeled in the approximation of axial symmetry of the flame is a criterion for the research results reliability.

The Gauss-Newton method application [5, 6] is proposed to iterative algorithm optimize for reconstructing the phase function in Hilbert diagnostics in this paper. This is an iterative

numerical method for solving the least squares problem, a Newton's method modification for finding the objective function minimum. It does not require the second derivatives definition, unlike Newton's method, which greatly simplifies and reduces the calculations number [7]. Various modifications of the Gauss-Newton method that increase the convergence rate and reduce of the ill-posedness influence in the formulation problem (in particular, the Levenberg-Marquardt algorithm [8]) are presented in [9–11]. The Gauss-Newton method is effective in solving many optimization problems, it is easy to implement and is present in most software packages for applied mathematics.

2. Inverse problem of phase function reconstructing from hilbertograms

Let us turn to Fig. 1, where the selected section \hat{y} of the studied phase object with a radial distribution of the refractive index $n(r)$ is shown in a simplified way, the z axis coincides with the direction of the probing light beam.

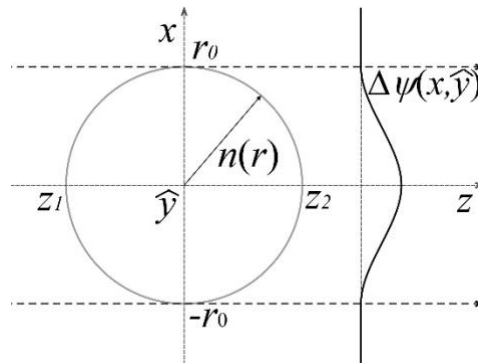


Fig. 1. Scheme for diagnosing a phase object (axisymmetric approximation):
 $n(r)$ – radial distribution of the refractive index.

Phase perturbations $\Delta\psi(x, \hat{y})$ of the probing light field that has passed through the medium under study depend on the geometric path length and the refractive index $n(x, \hat{y}, z)$:

$$\Delta\psi(x, \hat{y}) = \frac{2\pi}{\lambda} \int_{z_1}^{z_2} [n(x, \hat{y}, z) - n_\infty] dz,$$

where λ is the wavelength, n_∞ is the refractive index of air, z_1 and z_2 are the entry and exit points of the beam from the object.

The nonlinear integral operator of the first kind is a mathematical model of the Hilbert visualization of the phase shift $\Delta\psi(x, \hat{y})$:

$$H[\Delta\psi](x^*, \hat{y}) = \left\{ \int_{-\infty}^{+\infty} \frac{\cos[\Delta\psi(x, \hat{y})]}{x^* - x} dx \right\}^2 + \left\{ \int_{-\infty}^{+\infty} \frac{\sin[\Delta\psi(x, \hat{y})]}{x^* - x} dx \right\}^2. \quad (1)$$

The inverse problem consists in reconstructing the function $\Delta\psi(x, \hat{y})$ from the $H[\Delta\psi](x^*, \hat{y})$ values, which are recorded in the experiment.

The method based on the successive selection of the profile $\Delta\psi(x, \hat{y})$ and calculation of the hilbertogram $H[\Delta\psi](x^*, \hat{y})$ is proposed for the solution. The local extrema coincidence of the experimental and reconstructed hilbertograms serves as a criterion for stopping the procedure.

The desired phase perturbation function $\Delta\psi(x, \hat{y})$ in the section \hat{y} on the interval $[-r_0, r_0]$ is modeled by Bernstein polynomials of the n -th order (Bezier curves) in the smooth fields case [12]:

$$\Delta\psi(x, \hat{y}) = \begin{cases} x(t, P_x) = \sum_{m=0}^n P_{x,m} b_{m,n}(t) \\ y(t, P_y) = \sum_{m=0}^n P_{y,m} b_{m,n}(t) \end{cases}; \quad t \in [0,1]; \quad (2)$$

where $(P_{x,m}, P_{y,m})$ are the vectors components of the reference vertexes, $b_{m,n}(t)$ are the basis functions of the Bezier curve, called Bernstein polynomials:

$$b_{m,n}(t) = \frac{n!}{m!(n-m)!} t^m (1-t)^{n-m},$$

n is the polynomial degree, m is the ordinal number of the reference vertex. The function $\Delta\psi(x, \hat{y}) = 0$ outside the interval $[-r_0, r_0]$.

The equality $\Delta\psi[x(t), \hat{y}] = y(x(t))$ is valid in the section \hat{y} for the phase function (2) and any parameter t , while $\Delta\psi(x, \hat{y})$ depends on the coordinates of the reference points \vec{P} . Denote its Hilbert image by $H_{\vec{P}}^{opt}$. It is calculated taking into account formula (1) as follows:

$$H_{\vec{P}}^{opt}[y](x^*) = \left\{ \int_{-r_0}^{r_0} \frac{\cos[y(x)]}{x^* - x} dx \right\}^2 + \left\{ \int_{-r_0}^{r_0} \frac{\sin[y(x)]}{x^* - x} dx \right\}^2. \quad (3)$$

As $dx = x'_t(t, P_x) dt$, where $x'_t = dx/dt$, equation (3) can be represented as

$$H_{\vec{P}}^{opt}[y](x^*) = \left\{ \int_0^1 \frac{\cos[y(t, P_y)]}{x^* - x(t, P_x)} x'_t(t, P_x) dt \right\}^2 + \left\{ \int_0^1 \frac{\sin[y(t, P_y)]}{x^* - x(t, P_x)} x'_t(t, P_x) dt \right\}^2. \quad (4)$$

The optimization problem is to determine those values of the parameters $(P_{x,0}, \dots, P_{x,n})$ and $(P_{y,0}, \dots, P_{y,n})$, at which the objective function minimum is reached:

$$f(\vec{P}) = \|F(\vec{P})\|^2 = \sum_{k=0}^N [H^{ref}(x_k) - H_{\vec{P}}^{opt}(x_k)]^2, \quad x_k \in [-r_0, r_0], \quad (5)$$

where H^{ref} is the hilbertogram recorded in the experiment (reference data).

3. Gauss-Newton method

In general terms, the optimization problem is to find the extremum (minimum) of the objective function:

$$f(\vec{u}) = \|F(\vec{u})\|^2 = \sum_{k=0}^N [a_k(\vec{u}) - b_k]^2, \\ \vec{u} = (u_1, \dots, u_m) \in \mathbb{R}^m.$$

The iterative Gauss-Newton method, which uses the Jacobian matrix J of first-order derivatives of the function $F(\vec{u})$ to find the vector \vec{u}_* that minimizes $f(\vec{u})$, is one way to solve this problem.

The Jacobian matrix is determined by the formula [13, 14]:

$$J(\vec{u}) = \left[\frac{\partial a_k(\vec{u})}{\partial u_j} \right]_{k=1, j=1}^{N, m}.$$

The Gauss-Newton method consists in performing successive approximations \vec{u}_{d+1} according to the expression:

$$\vec{u}_{d+1} = \vec{u}_d - \alpha [J^T(\vec{u}_d) J(\vec{u}_d)]^{-1} J^T(\vec{u}_d) F(\vec{u}_d), \quad (6)$$

where d is the iteration number, α is the coefficient used to regulate the optimization "step" [6], J^T is the transposed matrix.

Denote

$$H_k^{ref} = H^{ref}(x_k), \quad H_k^{opt}[y(x(t, P_x), P_y)] = H_{\vec{P}}^{opt}(x_k).$$

Then the objective function components (5) in the case of hilbertogram processing can be written as

$$F = \begin{Bmatrix} H_0^{ref} - H_0^{opt}[y(x(t, P_x), P_y)] \\ \vdots \\ H_N^{ref} - H_N^{opt}[y(x(t, P_x), P_y)] \end{Bmatrix}. \quad (7)$$

The partial derivatives values with respect to the components of the vector \vec{P} of the function (4) will be found to determine the Jacobi matrix J . First, we write down the values of derivatives with respect to P_x coordinates:

$$\frac{\partial H^{opt}}{\partial P_x}(x^*) = \left| \left\{ \int_0^1 \frac{\cos[y(t, P_y)]}{x^* - x(t, P_x)} x'_t(t, P_x) dt \right\}^2 \right|'_{P_x} + \left| \left\{ \int_0^1 \frac{\sin[y(t, P_y)]}{x^* - x(t, P_x)} x'_t(t, P_x) dt \right\}^2 \right|'_{P_x} = A_x + B_x.$$

Then

$$A_x = 2 \int_0^1 \frac{\cos[y(t, P_y)]}{x^* - x(t, P_x)} x'_t(t, P_x) dt \cdot \left| \int_0^1 \frac{\cos[y(t, P_y)]}{x^* - x(t, P_x)} x'_t(t, P_x) dt \right|'_{P_x}.$$

Since

$$\left| \frac{\cos[y(t, P_y)]}{x^* - x(t, P_x)} x'_t(t, P_x) dt \right|'_{P_x} = \cos[y(t, P_y)] \left| \frac{x'_t(t, P_x)}{x^* - x(t, P_x)} \right|'_{P_x},$$

and

$$\left| \frac{x'_t(t, P_x)}{x^* - x(t, P_x)} \right|'_{P_x} = \frac{|x'_t(t, P_x)|'_{P_x} \cdot [x^* - x(t, P_x)] - x'_t(t, P_x) \cdot |x^* - x(t, P_x)|'_{P_x}}{[x^* - x(t, P_x)]^2},$$

it follows that

$$\left| \frac{\cos[y(t, P_y)]}{x^* - x(t, P_x)} x'_t(t, P_x) dt \right|'_{P_x} = \cos[y(t, P_y)] \frac{w_1 \cdot [x^* - x(t, P_x)] + w_2 \cdot x'_t(t, P_x)}{[x^* - x(t, P_x)]^2},$$

where

$$w_1 = |x'_t(t, P_x)|'_{P_x}, \\ w_2 = -|x^* - x(t, P_x)|'_{P_x} = |x(t, P_x)|'_{P_x}.$$

Thus

$$A_x = 2 \int_0^1 \frac{\cos[y(t, P_y)]}{x^* - x(t, P_x)} x'_t(t, P_x) dt \cdot \left\{ \int_0^1 \frac{\cos[y(t, P_y)]}{x^* - x(t, P_x)} w_1 dt + \int_0^1 \frac{\cos[y(t, P_y)]}{[x^* - x(t, P_x)]^2} w_2 \cdot x'_t(t, P_x) dt \right\},$$

or

$$A_x = \{I_1 + I_2\} \cdot 2 \int_{-r_0}^{r_0} \frac{\cos[y(x)]}{x^* - x} dx,$$

where

$$I_1 = \int_{-r_0}^{r_0} \frac{\cos[y(x)]}{x^* - x} \cdot \frac{w_1}{x'_t(t, P_x)} dx, \\ I_2 = \int_{-r_0}^{r_0} \frac{\cos[y(x)]}{[x^* - x]^2} \cdot w_2 dx. \quad (8)$$

We transform (8) by integration by parts:

$$I_2 = - \int_{-r_0}^{r_0} \frac{|\cos[y(x)] \cdot w_2|'_x}{x^* - x} dx.$$

Since

$$|\cos[y(x)] \cdot w_2|'_x = |\cos[y(x)]|'_x \cdot w_2 + \cos[y(x)] \cdot |w_2|'_x, \\ |\cos[y(x)]|'_x = -\sin[y(x)] \frac{y'_t(t, P_y)}{x'_t(t, P_x)},$$

$$|w_2|'_x = \frac{|w_2|'_t}{x'_t(t, P_x)} = \frac{w_1}{x'_t(t, P_x)},$$

then

$$I_2 = \int_{-r_0}^{r_0} \frac{\sin[y(x)]}{x^* - x} \cdot \frac{y'_t(t, P_y)}{x'_t(t, P_x)} \cdot w_2 dx - \int_{-r_0}^{r_0} \frac{\cos[y(x)]}{x^* - x} \cdot \frac{w_1}{x'_t(t, P_x)} dx.$$

As a result, we arrive at the equality

$$\begin{aligned} A_x &= 2 \int_{-r_0}^{r_0} \frac{\cos[y(x)]}{x^* - x} dx \left\{ \int_{-r_0}^{r_0} \frac{\cos[y(x)]}{x^* - x} \cdot \frac{w_1}{x'_t(t, P_x)} dx + \right. \\ &+ \left. \int_{-r_0}^{r_0} \frac{\sin[y(x)]}{x^* - x} \cdot \frac{y'_t(t, P_y)}{x'_t(t, P_x)} \cdot w_2 dx - \int_{-r_0}^{r_0} \frac{\cos[y(x)]}{x^* - x} \cdot \frac{w_1}{x'_t(t, P_x)} dx \right\} = \\ &= 2 \int_{-r_0}^{r_0} \frac{\cos[y(x)]}{x^* - x} dx \int_{-r_0}^{r_0} \frac{\sin[y(x)]}{x^* - x} \cdot \frac{y'_t(t, P_y)}{x'_t(t, P_x)} \cdot w_2 dx. \end{aligned}$$

Similarly, one can show that

$$B_x = -2 \int_{-r_0}^{r_0} \frac{\sin[y(x)]}{x^* - x} dx \int_{-r_0}^{r_0} \frac{\cos[y(x)]}{x^* - x} \cdot \frac{y'_t(t, P_y)}{x'_t(t, P_x)} \cdot w_2 dx.$$

Now we write down the values of derivatives with respect to P_y coordinates:

$$\begin{aligned} \frac{\partial H^{opt}}{\partial P_y}(x^*) &= \left\{ \int_0^1 \frac{\cos[y(t, P_y)]}{x^* - x(t, P_x)} x'_t(t, P_x) dt \right\}^2 \Big|_{P_y}' + \left\{ \int_0^1 \frac{\sin[y(t, P_y)]}{x^* - x(t, P_x)} x'_t(t, P_x) dt \right\}^2 \Big|_{P_y}' = \\ &= A_y + B_y. \end{aligned}$$

Then

$$A_y = 2 \int_0^1 \frac{\cos[y(t, P_y)]}{x^* - x(t, P_x)} x'_t(t, P_x) dt \left| \int_0^1 \frac{\cos[y(t, P_y)]}{x^* - x(t, P_x)} x'_t(t, P_x) dt \right|_{P_y}'.$$

Since

$$\begin{aligned} \left| \frac{\cos[y(t, P_y)]}{x^* - x(t, P_x)} x'_t(t, P_x) \right|_{P_y}' &= \frac{x'_t(t, P_x)}{x^* - x(t, P_x)} \cdot |\cos[y(t, P_y)]|'_{P_y}, \\ |\cos[y(t, P_y)]|'_{P_y} &= -\sin[y(t, P_y)] \cdot w_2, \end{aligned}$$

we get

$$A_y = -2 \int_0^1 \frac{\cos[y(t, P_y)]}{x^* - x(t, P_x)} x'_t(t, P_x) dt \int_0^1 \frac{\sin[y(t, P_y)]}{x^* - x(t, P_x)} x'_t(t, P_x) \cdot w_2 dt,$$

or

$$A_y = -2 \int_{-r_0}^{r_0} \frac{\cos[y(x)]}{x^* - x} dx \int_{-r_0}^{r_0} \frac{\sin[y(x)]}{x^* - x} \cdot w_2 dx.$$

Similarly

$$B_y = 2 \int_{-r_0}^{r_0} \frac{\sin[y(x)]}{x^* - x} dx \int_{-r_0}^{r_0} \frac{\cos[y(x)]}{x^* - x} \cdot w_2 dx.$$

As a result, the Jacobian matrix will have the following form:

$$J = \begin{Bmatrix} \frac{\partial H_0^{opt}}{\partial P_{x,0}} & \dots & \frac{\partial H_0^{opt}}{\partial P_{x,n}} & \frac{\partial H_0^{opt}}{\partial P_{y,0}} & \dots & \frac{\partial H_0^{opt}}{\partial P_{y,n}} \\ \vdots & \ddots & \vdots & \vdots & \ddots & \vdots \\ \frac{\partial H_N^{opt}}{\partial P_{x,0}} & \dots & \frac{\partial H_N^{opt}}{\partial P_{x,n}} & \frac{\partial H_N^{opt}}{\partial P_{y,0}} & \dots & \frac{\partial H_N^{opt}}{\partial P_{y,n}} \end{Bmatrix}. \quad (9)$$

The Gauss-Newton algorithm (6), taking into account (7) and (9), will be defined as

$$\overrightarrow{P_{d+1}} = \overrightarrow{P_d} - \alpha [J^T J]^{-1} J^T F(\overrightarrow{P_d}). \quad (10)$$

Thus, optimization begins with setting the vector components \vec{P}_0 , which determine the phase function initial profile, then applying formula (10) step by step, and terminating the calculation process when the squared distances sum between the extrema coordinates of the reference and optimized hilbertograms becomes less than the specified value.

4. Algorithm application on the test function example

It is sufficient to determine the phase function only on the interval $[0, r_0]$ in the case of axisymmetric objects.

Let's simulate an example when an axisymmetric object with a section radius $r_0 = 30$ mm is diagnosed. Define $\Delta\psi(x, \hat{y})$ within $0 \leq x \leq r_0$ as a parametric Bezier curve of the third degree:

$$\Delta\psi(x, \hat{y}) = \begin{cases} x(t) = (1-t)^3 P_{x,0} + 3(1-t)^2 t P_{x,1} + 3(1-t)t^2 P_{x,2} + t^3 P_{x,3} \\ y(t) = (1-t)^3 P_{y,0} + 3(1-t)^2 t P_{y,1} + 3(1-t)t^2 P_{y,2} + t^3 P_{y,3} \end{cases}$$

for $x \geq r_0$ the value $\Delta\psi(x, \hat{y}) = 0$, and we continue it in an even way to the region $-r_0 \leq x \leq 0$.

The pixel size in the image corresponded to $1/30$ mm when registering the optical signal in the experiments [3, 4]. Therefore, the number of samples $N = 1801$ in the interval $[-r_0, r_0]$.

The function graph $\Delta\psi(x, \hat{y})$ and its hilbertogram is shown in Fig. 2 for the reference points values

$$\{P_{x,0} = 0, P_{y,0} = 50\}, \{P_{x,1} = 15, P_{y,1} = 50\}, \{P_{x,2} = 15, P_{y,2} = 0\}, \\ \{P_{x,3} = 30, P_{y,3} = 0\}.$$

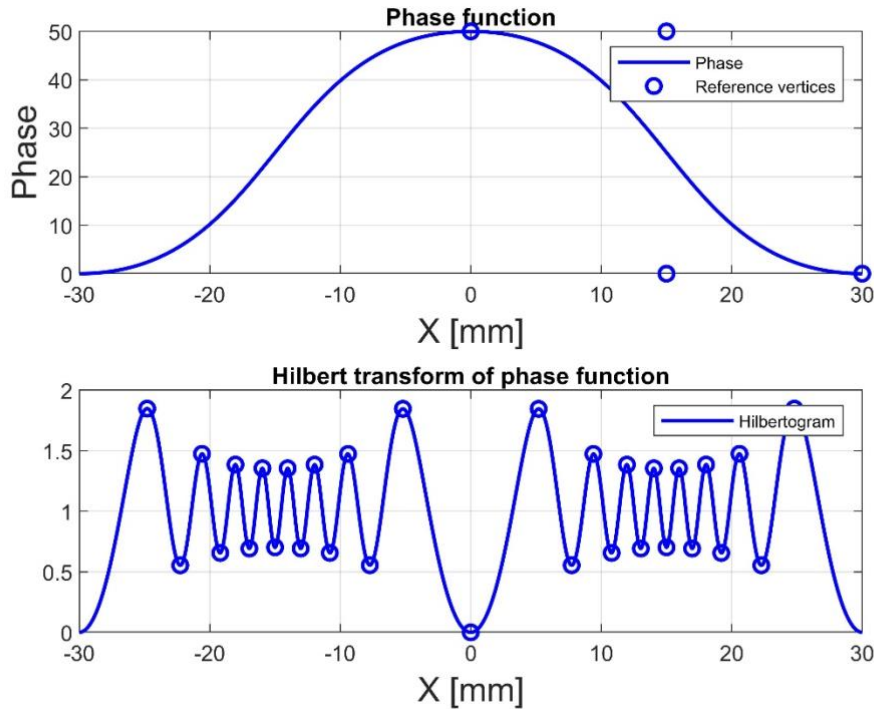


Fig. 2. The phase function represented by the Bezier curve (with reference vertices) and the hilbertogram calculated from it. The hilbertogram is presented in a dimensionless form with indication of the local extrema points.

The hilbertogram shown in Fig. 2 will be taken as the reference H^{ref} , and the phase function corresponding to it will be denoted by $\Delta\psi^{ref}$. Let us consider the biased function H^{opt} as an initial approximation, which must be optimized to H^{ref} (Fig. 3).

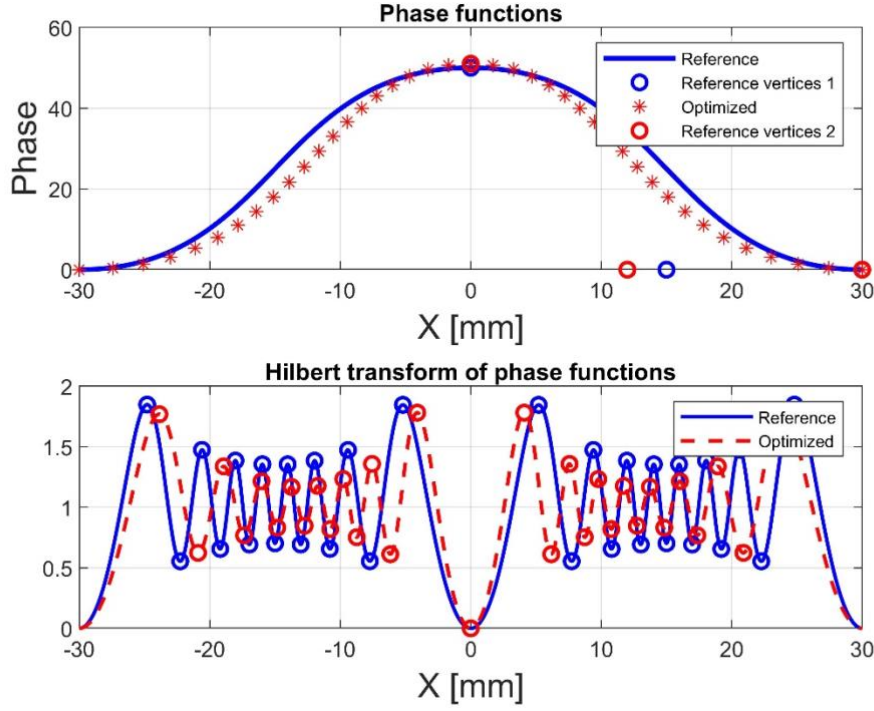


Fig. 3. Reference hilbertogram H^{ref} and initial (optimized) hilbertogram H^{opt} , and their corresponding phase functions.

In this case, the parameter w_2 for derivatives with respect to the vector \vec{P} will have the values presented in Table 1.

Table 1. Derivatives with respect to P_x and P_y coordinates

Coordinates P_x	Coordinates P_y	w_2
$P_{x,0}$	$P_{y,0}$	$(1-t)^3$
$P_{x,1}$	$P_{y,1}$	$3(1-t)^2t$
$P_{x,2}$	$P_{y,2}$	$3(1-t)t^2$
$P_{x,3}$	$P_{y,3}$	t^3

The Jacobian matrix will have the following form:

$$J = \left\{ \begin{array}{cccccccc} \frac{\partial H_0^{opt}}{\partial P_{x,0}} & \frac{\partial H_0^{opt}}{\partial P_{x,1}} & \frac{\partial H_0^{opt}}{\partial P_{x,2}} & \frac{\partial H_0^{opt}}{\partial P_{x,3}} & \frac{\partial H_0^{opt}}{\partial P_{y,0}} & \frac{\partial H_0^{opt}}{\partial P_{y,1}} & \frac{\partial H_0^{opt}}{\partial P_{y,2}} & \frac{\partial H_0^{opt}}{\partial P_{y,3}} \\ \vdots & \vdots & \vdots & \vdots & \vdots & \vdots & \vdots & \vdots \\ \frac{\partial H_N^{opt}}{\partial P_{x,0}} & \frac{\partial H_N^{opt}}{\partial P_{x,1}} & \frac{\partial H_N^{opt}}{\partial P_{x,2}} & \frac{\partial H_N^{opt}}{\partial P_{x,3}} & \frac{\partial H_N^{opt}}{\partial P_{y,0}} & \frac{\partial H_N^{opt}}{\partial P_{y,1}} & \frac{\partial H_N^{opt}}{\partial P_{y,2}} & \frac{\partial H_N^{opt}}{\partial P_{y,3}} \end{array} \right\}.$$

The root-mean-square error between the hilbertogram H^{ref} and H^{opt} after 30 iterations as a result of applying the Gauss-Newton method (10) has reached the value

$$\sigma_{cp} = \sqrt{\sum_{k=0}^N (H_k^{opt} - H_k^{ref})^2} = 0,09,$$

while the maximum deviation was

$$\sigma_{max} = \max_{k=0,\dots,N} |H_k^{opt} - H_k^{ref}| = 0,005.$$

The phase function $\Delta\psi^{opt}$ obtained as a result of optimization is shown in Fig. 4.

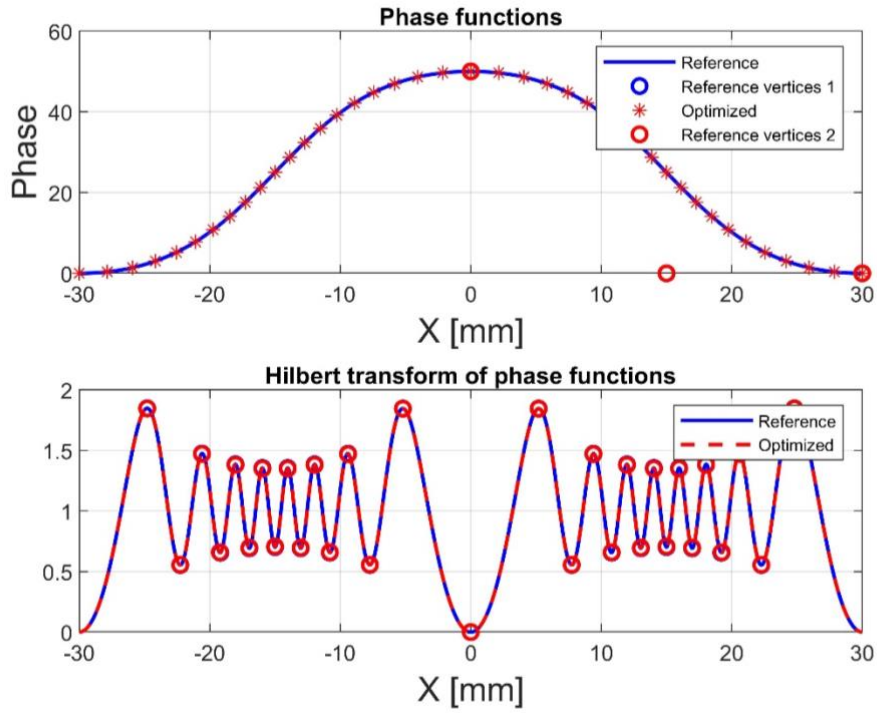
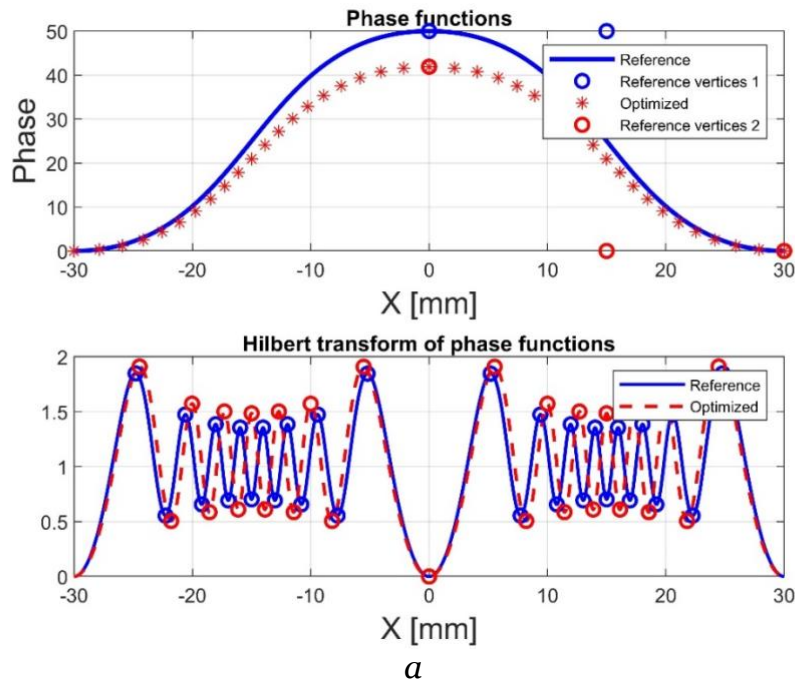


Fig. 4. Optimization result.

The maximum deviation of $\Delta\psi_{opt}$ from $\Delta\psi_{ref}$ was

$$\sigma_{max}(\Delta\psi) = \max_{k=0,\dots,N} |\Delta\psi_k^{opt} - \Delta\psi_k^{ref}| = 0,01.$$

The initial approximation H^{opt} in the considered example was chosen in such a way that the number of Hilbert bands H^{ref} and H^{opt} coincided. Let's try to estimate the “limit” deviation of the initial approximation H^{opt} , at which the Gauss-Newton algorithm begins to work incorrectly (Fig. 5 and 6).



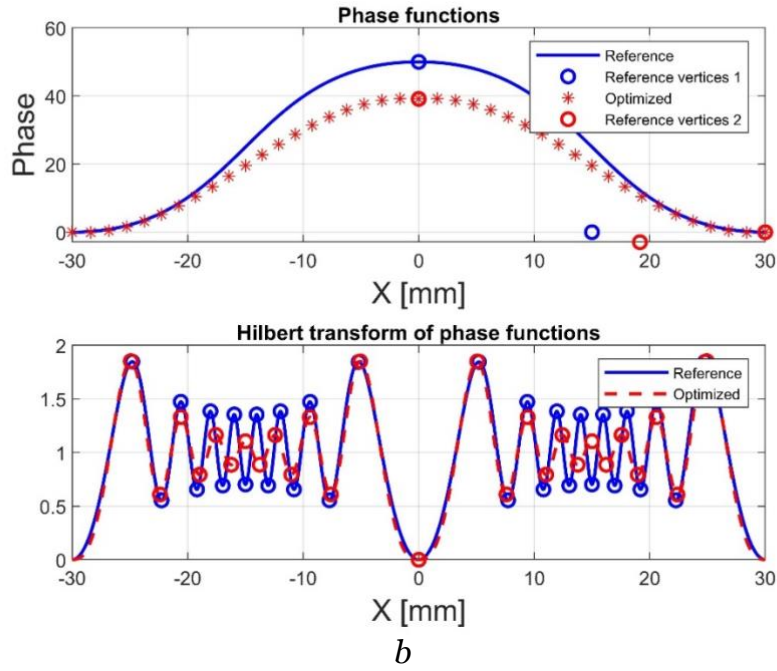


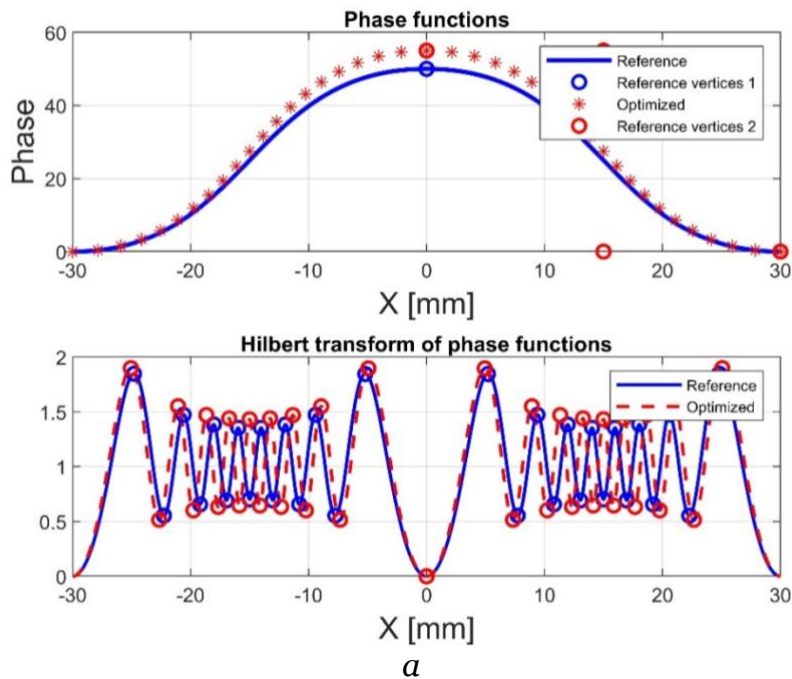
Fig. 5. (a) – Reference hilbertogram H^{ref} and initial (optimized) hilbertogram H^{opt} , and their corresponding phase functions (second approximation); (b) – optimization result.

Let the initial approximation H^{opt} be smaller by one Hilbert band in the ranges $[-r_0; 0]$ and $[0; r_0]$ than the hilbertogram H^{ref} (as shown in Fig. 5.a). As a result, the following values were achieved after 12 iterations (Fig. 5.b):

$$\sigma_{cp} = \sqrt{\sum_{k=0}^N (H_k^{opt} - H_k^{ref})^2} = 6,54, \quad \sigma_{max} = \max_{k=0, \dots, N} |H_k^{opt} - H_k^{ref}| = 0,45,$$

$$\sigma_{max}(\Delta\psi) = \max_{k=0, \dots, N} |\Delta\psi_k^{opt} - \Delta\psi_k^{ref}| = 10,88.$$

Now let's set the H^{opt} so that the number of Hilbert bands is greater by one in the same ranges $[-r_0; 0]$ and $[0; r_0]$ (Fig. 6.a).



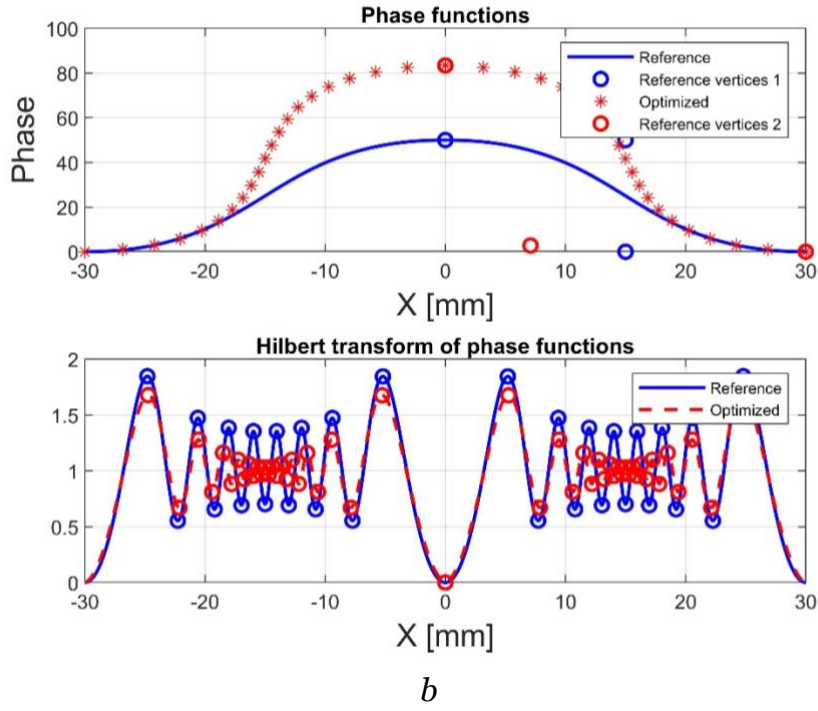


Fig. 6. (a) – Reference hilbertogram H^{ref} and initial (optimized) hilbertogram H^{opt} , and their corresponding phase functions (third approximation); (b) – optimization result.

As a result, after 41 iterations we obtained (Fig. 6.b):

$$\sigma_{cp} = \sqrt{\sum_{k=0}^N (H_k^{opt} - H_k^{ref})^2} = 6,85, \quad \sigma_{max} = \max_{k=0, \dots, N} |H_k^{opt} - H_k^{ref}| = 0,46,$$

$$\sigma_{max}(\Delta\psi) = \max_{k=0, \dots, N} |\Delta\psi_k^{opt} - \Delta\psi_k^{ref}| = 33,38.$$

Thus, it was found that for the convergence of the Gauss-Newton algorithm it is necessary that the number of Hilbert bands H^{opt} and H^{ref} be equal. In practice, of course, it is necessary that the Hilbert bands of the experimental and optimized hilbertograms be as “close” to each other as possible.

5. Conclusion

The Gauss-Newton method is adapted to the problem of phase function determining from Hilbert diagnostic data of gaseous, condensed and reacting media. The phase structure reconstruction algorithm is based on the sequential selection of the phase profile specified by the Bézier polynomial and subsequent calculation of the hilbertogram. The local extrema coincidence of the reference and reconstructed hilbertograms is a criterion for the results reliability. The Jacobian matrix calculation for the nonlinear integral operator of Hilbert visualization has been completed, and an operation example of the algorithm for the test function in the case of an axisymmetric formulation of the problem is given.

Direction of further research: application of the algorithm to the experimental data processing. Adaptation of the Gauss-Newton method to the possibility of specifying the desired phase function using several Bezier curves in cases of diagnosing complex structures.

The work of the first author was carried out within the framework of the state assignment of IM SB RAS (No. FWNF-2022-0009), and the work of the other authors was carried out within the framework of the state assignment of IT SB RAS (No. 121031800217-8).

References

1. Arbuzov V. A., Dubnishchev Yu. N. *Metody gil'bert-optiki v izmeritel'nykh tekhnologiyakh* [Hilbert-optics methods in measurement technologies], NSTU University Publ., Novosibirsk, 2007, 316 p. (in Russian)
2. Soroko L. M. *Gil'bert-optika* [Hilbert optics], Nauka Publ., Moscow, 1981, 160 p. (in Russian)
3. Arbuzov V. A., Arbuzov E. V., Dubnishchev Yu. N., Lukashov V. V., Zolotukhina O. S. Method of polychromatic Hilbert diagnostics of phase and temperature perturbations of axisymmetric flames // *CEUR Workshop Proceedings*, Vol. 3027, 2021, pp. 369–378 (doi: 10.20948/graphicon-2021-3027-369-378).
4. Arbuzov V. A., Arbuzov E. V., Dubnishchev Yu. N., Lukashov V. V., Zolotukhina O. S., Tupikin A. V. Hilbert-optic diagnostics of hydrogen-oxygen inverse diffusion flame // *Energies*, Vol. 15 (24), 2022, P. 9566 (doi: 10.3390/en15249566).
5. Floudas C. A., Pardalos P. M. *Encyclopedia of optimization*. New York: Springer, 2008, 4622 p.
6. Levenberg-Marquardt algorithm for non-linear least squares method and its implementation in Python, 2016. URL: <http://habr.com/ru/articles/308626/>.
7. Lovetsky K. P., Sevastyanov L. A., Bikeev O. N., Pauksho M. V. *Matematicheskiy sintez opticheskikh nanostruktur* [Mathematical synthesis of optical nanostructures], RUDN University Publ., Moscow, 145 p. (in Russian)
8. Vasin V. V. The Levenberg-Marquardt method for approximation of solutions of irregular operator equations // *Automation and remote control*, Vol. 73, 2012, pp. 440–449 (doi: 10.1134/S0005117912030034).
9. Yudin N. E. Modified Gauss–Newton method for solving a smooth system of nonlinear equations // *Computer research and modeling*, Vol. 13, pp. 2021, pp. 697–723 (doi: 10.20537/2076-7633-2021-13-4-697-723).
10. Loke M. H., Dahlin T. A comparison of the Gauss-Newton and quasi-Newton methods in resistivity imaging inversion // *Journal of Applied Geophysics*, Vol. 49 (3), 2002, pp. 149–162 (doi: 10.1016/S0926-9851(01)00106-9).
11. Bergou E. H., Diouane Y., Kungurtsev V. Convergence and complexity analysis of a Levenberg-Marquardt algorithm for inverse problems // *Journal of Optimization Theory and Applications*, Vol. 185, 2020, pp. 927–944 (doi: 10.1007/s10957-020-01666-1).
12. Rogers D. F., Adams J. A. *Mathematical elements for computer graphics* (Second Edition), McGraw-Hill, New York, 1990.
13. Zorich V. A. *Matematicheskiy analiz* [Mathematical analysis], part 1, 6st. ed., ICNMO Publ., Moscow, 2012, 702 p. (in Russian)
14. Bakhvalov N. S., Zhidkov N. P., Kobelkov G. M. *Chislennyye metody* [Numerical methods], Binom Publ., Moscow, 2003, 632 p. (in Russian)